Measured effects of shock waves on supersonic hydrogen-air flames

Hwanil Huh
Michigan Univ., Ann Arbor

James F. Driscoll
Michigan Univ., Ann Arbor

AIAA, ASME, SAE, and ASEE, Joint Propulsion Conference and Exhibit, 32nd, Lake Buena Vista, FL, July 1-3, 1996

A supersonic nonpremixed jet-like flame was stabilized along the axis of a Mach 2.5 wind tunnel, and wedges were mounted on the sidewall in order to interact oblique shock waves with the flame. It was found that shock waves enhance the fuel-air mixing such that flame lengths decreased by 30 percent when an optimum shock location and shock strength were chosen. Enhanced mixing resulted, in part, because the shocks turn the flow and induce radial inflows of air into the fuel jet. Substantial improvements in flame stability was achieved by properly interacting the shock waves with the flameholding recirculation zone. The reason for the significant improvement in flame stability is believed to be the adverse pressure gradient caused by the shock, which can elongate the recirculation zone. Optimization of the mixing and stability limits requires a careful matching of the shock-flame interaction location and the shock strength. The results show that the best mixing and stability corresponds to 10-deg wedges placed at an upstream position such that the primary shocks create radial inflow near the flame base and interact with the recirculation zone. (Author)

MEASURED EFFECTS OF SHOCK WAVES ON SUPERSONIC HYDROGEN-AIR FLAMES

Hwanil Huh[*] and James F. Driscoll[†]
The University of Michigan, Ann Arbor, MI 48105

Abstract

A supersonic nonpremixed, jet-like flame was stabilized along the axis of a Mach 2.5 wind tunnel, and wedges were mounted on the sidewall in order to interact oblique shock waves with the flame. This experiment was the first reacting flow experiment interacting with shock waves. It was found that shock waves enhance the fuel-air mixing such that flame lengths decreased by 30% when an optimum shock location and shock strength was chosen. Enhanced mixing resulted, in part, because the shocks turn the flow and induce radial inflows of air into the fuel jet. Substantial improvements in the flame stability were achieved by properly interacting the shock waves with the flameholding recirculation zone. The reason for the significant improvement in flame stability is believed to be the adverse pressure gradient caused by the shock, which can elongate the recirculation zone. Optimization of the mixing and stability limits requires a careful matching of the shock-flame interaction location and the shock strength. The results show that the best mixing and stability corresponds to an $10°$ wedges placed at an upstream position such that the primary shocks create radial inflow near the flame base and interact with the recirculation zone.

Nomenclature

d_F = fuel tube inner diameter (0.70cm)
m = mass flow rate
P_{pitot} = pitot pressure
P_W = wall static pressure
X = streamwise coordinate
Y = transverse coordinate
Z = spanwise coordinate
γ = specific heat ratio
ρ = density
ω = vorticity

Subscript

1 = upstream
A = air
F = fuel
f = flame
o = stagnation

Introduction

Oblique shock waves that form within a scramjet combustor are often unavoidable; if the waves are sufficiently oblique to the flow their stagnation pressure losses are not appreciable yet they may have the positive effects of enhancing the fuel-air mixing and helping to stabilize the flame base. The purpose of the present work is to quantify and optimize certain beneficial effects of oblique shock waves on a supersonic jet-like flame.

In general, shock waves can affect a flame because they can (a) direct the airflow radially inward (toward the fuel) and thus increase the air entrainment rate, (b) create additional vorticity[1] which enhances the mixing rates, (c) create an adverse pressure gradient which elongates recirculation zones or creates new separation zones[2] and (d) increase the static pressure, static temperature and reaction rates. The present supersonic flame was stabilized along the axis of a Mach 2.5 wind tunnel using a thick-lipped fuel tube that acts as a bluff-body. Two identical small wedges on the tunnel sidewalls create oblique planar shocks and the optimum position of the shock-flame interaction and the optimum shock strength were investigated. This work is an extension of recent studies in our laboratory of supersonic jet flames with no shock waves[3,4]. Previously, Winterfeld[2] interacted an oblique shock with a supersonic jet flame for a limited set of conditions and reported some preliminary results showing that the shock improved the flame blowout limits. Little else appears in the archival literature concerning a shock wave interacting with a turbulent jet flame. Related studies have considered a shock wave

---

[*] Graduate Student Instructor, Department of Aerospace Engineering, Student Member AIAA
[†] Professor, Department of Aerospace Engineering, Senior Member AIAA

interacting with a reacting shear layer, as reported by Menon[5] and Drummond et al.[6]. Numerous studies have considered nonreacting flows that interact with shock waves; for example, the well-known work of Marble[1], Yang et al.[7], and Jacobs[8] considers a laminar, circular jet of helium that is distorted by shock-generated vorticity. Other related nonreacting flow studies involved shock waves interacting with a contoured wall injector, as described by Waitz et al.[9] and Eklund et al.[10]. Nonreacting vortex rings were distorted by shock waves, as reported by Cetegen and Hermanson[11], and the effects of shocks on a nonreacting jet in a crossflow were described by Heister and Karagozian[12]. Cheuch et al.[13], Glawe et al.[14], and Barlow et al.[15] have quantified the mixing in nonreacting underexpanded sonic jets having cellular shock patterns. A useful description of the reacting supersonic jet flame itself (with no shock waves) is provided by the data of Cheng, et al.[16]. One of the most pronounced effects of shock waves on fuel-air mixing has been identified by Marble[1], who showed that baroclinic torques can create shock-generated vorticity. This shock-generated vorticity has a large effect on a laminar jet[1,2,3] which has a relatively small amount of initial vorticity and has a relatively low fuel-air mixing rate. However, it is realized that shock-generated vorticity is expected to have a smaller effect on the present turbulent jet (than that reported for the laminar jet) because the high-speed turbulent jet inherently has a relatively large amount of vorticity.

Experimental Methods

A schematic of the experiment appears in Figure 1. A jet-like flame is stabilized on the axis of a Mach 2.5 wind tunnel using a thick-lipped fuel tube which acts as a bluff body. Air is expanded to Mach 2.5 using a 2-D nozzle that was designed using the method of characteristics; the combustor is 55 cm long and 5.7 cm by 4.1 cm at the fuel injection location. Two of the combustor sidewalls are parallel while the other two diverge at 4° from the axis in order to prevent thermal choking. Each of the four stainless steel sidewalls has a quartz window for optical access. The facility is identical to that described in Refs. 3 and 4 except that larger windows were added and a more gradually contoured fuel tube is added which slightly changes the throat area.

The outside diameter of the fuel tube gradually changes from 2.54 cm at the end of the tube to 1.27 cm at the slightly upstream of the air nozzle throat, which is 24 cm upstream. The inside diameter (d_F) is 0.70 cm. Hydrogen is injected at sonic velocity and the fuel jet Reynolds number is typically 76,000. While the facility has an electrical air heater capable of heating the air to 1100 K, the stagnation temperature for all of the present flames is 285 K.

Three different wedges were used: wedge 1, wedge 2, wedge 3. Figure 2 illustrates a schematic of the shock-generating wedges. The first (Wedge 1) had an angle of 10 degrees and was considered a weak shock generator. The second (wedge 2) had an angle of 15 degrees and was a relatively strong shock generator. Finally, the third (wedge 3) had an angle of 20 degrees and considered a strong shock generator. Each wedge is 5.08 cm long and has a same thickness of 0.56 cm; otherwise, flow blockage ratio will be different. A 10° wedge consists of a 3.20 cm long slanted face aligned at 10° to the sidewall, followed by a 1.88 cm face that is parallel to the sidewall. Two identical wedges are mounted on the diverging sidewalls. The wedges span the entire 4.1 cm width of the combustor and are flushed with the sidewalls, producing a 2-D planar oblique shock free from any observable edge effects. In order to optimize shock-flame interaction, both the shock strength (wedge angle: 10°, 15°, 20°) and the location were varied.

Table 1 summarizes the change of flow properties across the oblique shock waves. The flow properties shown in the Table 1 were calculated with the shock wave relations. Across the oblique shock wave, the static pressure and static temperature increase; in the other hand, the stagnation pressure and Mach number decrease. As the shock strength (wedge angle) increases, local pressure and temperature increases significantly and local Mach number decreases, thereby may increase local reaction rate.

The location of a wedge (thus shock position) was varied. Table 2 lists position of wedge leading edge. Four different positions of the wedge leading edge (X_{wedge}) were used: upstream (1.0 d_F), mid-upstream (4.0 d_F), mid-downstream (8.5 d_F), and downstream (11.5 d_F).

Scaling Analysis

One important mechanism for mixing enhancement is expected to be the shock-induced-vorticity. Baroclinic torques can arise from the misalignment of density and pressure gradients across the shock wave. Therefore, it is of interest to estimate the relative magnitude of shock-induced-vorticity compared to inherent jet vorticity.

The rate of vorticity generation, $\dot{\omega}_{shock}$, due to shock waves is given by the baroclinic torque[1] term in the vorticity transport equation:

$$\dot{\omega}_{shock} = \frac{\Delta \omega_{shock}}{\Delta t_{shock}} = \frac{1}{\rho^2}\left|\vec{\nabla}\rho \times \vec{\nabla}P\right|$$
$$\cong \frac{1}{\rho_A^2}\left|\vec{\nabla}\rho\right| \cdot \left|\vec{\nabla}P\right| \cdot \sin\beta \tag{1}$$

where β is the interior angle measured between the density gradient vector $\overline{\nabla}\rho$ and the pressure gradient vector $\overline{\nabla}p$. β is taken to be positive if measured in the counter-clockwise direction (so that the right-hand rule holds). The magnitude of the density gradient can be approximated by

$$\left|\overline{\nabla}\rho\right| \cong \left(\rho_A - \rho_{H_2}\right)/\delta_{jet} \qquad (2)$$

where δ_{jet} is a characteristic halfwidth of the jet.

The magnitude of the pressure gradient can be approximated by

$$\left|\overline{\nabla}p\right| \cong \Delta p_{shock}/\Delta h_{shock} \qquad (3)$$

where Δh_{shock} is the thickness of the shock wave. The pressure change across the shock, ΔP_{shock}, is a function of the upstream Mach number M_1:

$$\frac{\Delta p_{shock}}{p_1} = \frac{2\gamma}{1+\gamma}\left\{\left(M_1 \sin\beta\right)^2 - 1\right\}$$
$$\cong \frac{2\gamma_A}{1+\gamma_A}\left\{\left(M_{1A} \sin\beta\right)^2 - 1\right\} \qquad (4)$$

As each fluid element crosses the shock wave, the vorticity that is added to each element will be $\dot{\omega}_{shock}$ multiplied by Δt_{shock}, which is the transit time to cross the shock wave. The transit time can be approximated as:

$$\Delta t_{shock} \cong \frac{\Delta h_{shock}}{U_1 \cdot \sin\beta} \qquad (5)$$

Equations (1) – (5) yield an expression for the amount of vorticity that is added just downstream of the shock wave:

$$\Delta\omega_{shock} \cong \dot{\omega}_{shock} \cdot \Delta t_{shock}$$
$$\cong \frac{1}{\rho_A^2}\frac{\left|\rho_A - \rho_{H_2}\right|}{\delta_{jet}}P_{1A}\frac{2\gamma_A}{1+\gamma_A}\left\{\left(M_{1A}\sin\beta\right)^2 - 1\right\}\frac{1}{U_{1A}} \qquad (6)$$

It is useful to compare the estimated vorticity generated by shock to the inherent vorticity in a turbulent jet:

$$\omega_{jet} \cong \Delta U/\delta_{jet} \qquad (7)$$

where ΔU is the jet centerline velocity minus the coflowing air velocity, and d_{jet} is the characteristic

halfwidth of the jet. Dividing equation (6) by equation (7) introduces a dimensionless "Vorticity Enhancement Parameter (VEP)" that gives the relative change in the vorticity of the inherent jet due to the effects of shock waves. This new parameter, VEP, will be defined by:

$$VEP \equiv \frac{shock-induced-vorticity}{inherent-jet-vorticity}$$
$$= \frac{\Delta\omega_{shock}}{\omega_{jet}}$$
$$\cong C_1\left(\sin^2\beta - \frac{1}{M_{1A}^2}\right)(1-s)\left(\frac{1}{1+r}\right) \qquad (8)$$

where C_1 (=4/(1+γ)) is a constant, s is the density ratio ρ_{H2}/ρ_A, and r is the speed ratio U_{Cl}/U_A. Equation (8) represents a relative vorticity enhancement due to shock interaction at one local point of shock-flow intersection. As a sample calculation, consider the typical experimental values; $\rho_F = 0.11$ kg/m^3, $\rho_A = 1.43$ kg/m^3, $U_F = 1191$ m/s, $U_A = 603$ m/s, $M_{1A} = 2.5$, wedge 2 ($\theta = 15°$, $\beta = 36.97°$). Equation (8) yields a value of VEP equal to 0.105; thus the shock induced vorticity is estimated to be about 10% of the inherent jet vorticity.

From equation (8), we can draw the following conclusions. A significant amount of new vorticity can be generated due to the shock interaction with the flame if one or more of the following four conditions are met.

1. The angle between the jet axis and the shock, β, is large (90° is the best).

A strong shock (having a large value of β) can generate a significant amount of new vorticity by creating a large amount of baroclinic torque. In the case of constant Mach number, strong shocks can be achieved by using large angle wedges. The significant temperature rise caused by the strong shocks can also lead to a rapid increase of the combustion efficiency right downstream of the shock interaction. On the other hand, this strong shock will also generate an undesired total pressure loss which negatively effects the SCRAMJET performance.

2. The upstream Mach number of air, M_{1A}, is large.

From Equation (8), VEP will be increased due to the $(\sin^2\beta - 1/M_{1A}^2)$ term as the upstream air Mach number M_{1A} is increased. Increased upstream air Mach number also leads to an increase of the air velocity as well as the shock deflection angle β, which increases the new vorticity generation as discussed above. However, since the shock deflection angle β is a function of the wedge angle (θ) as well as the upstream Mach number, the effect of upstream Mach number is complex. For this study, Mach number is 2.5 and minimum shock

3

deflection angle is 31.85° (wedge 1); therefore, the above statement is true.

3. The density ratio s, ρ_{H2}/ρ_A <1, is small.

The VEP will be increased due to the (1-s) term as the density ratio, s, is decreased. When density ratio decreases, density difference (density gradient) increases, thereby increases the new vorticity. A small density ratio can be achieved either by decreasing the hydrogen fuel density or by increasing the surrounding air density. For both cases, the supersonic flame length will be shorter. In other words, the new vorticity generation is more effective for the shorter flame length cases, which is not encouraging since in practical situations the flame length will be longer because of the low air density due to the high altitude.

4. The speed ratio r, U_{H2}/U_A >1, is small.

The VEP will be increased due to the $\{1/(1 + r)\}$ term as the speed ratio, r, is decreased. This speed ratio is determined by the design Mach numbers. A small speed ratio can be achieved by increasing the air temperature, and thus increasing the surrounding air flow speed. Since the speed ratio r is typically greater than unity, reducing r (but, still greater than unity) results in a smaller convective Mach number, M_c; which reduces the compressibility effect. The convective Mach number may also be reduced by the shock wave - flame interaction, which could result in a more unstable flow field. Thus, the vorticity fluctuations may be amplified by the instability mechanism.

EXPERIMENTAL RESULTS AND DISCUSSION

Figure 3 shows direct photographs and schlieren photographs of the supersonic flames with and without shock waves present. The upper flames shown in Figs. 3a, b, c, and f represent supersonic flames that interact with two planar oblique shock waves which are generated by the two 10° wedges (wedge 1) that are described in Figure 1. The location of the shock (leading edge of the wedge) is 4.0 d_F, the mid-upstream location. The lower flames in Figs. 3d, e, and h illustrate baseline supersonic flames with no wedges present. All photographs were taken with 0.5 s exposure time on ASA 1000 film with an f 2.8 aperture. Schlieren images of the nonreacting flow (with and without wedges) are shown in Fig. 3(i and j). The shocks appear more distinctly with no flame because the turbulent density gradients in the flame obscure the shocks within the flame. In addition, a special case is shown in Fig. 3g for which the wedge angle is

increased to 15° (wedge 2), resulting in thermal choking of the combustor, as described in Chapter 1. It can be concluded from Fig. 3 that as the fuel flow rate is increased, the supersonic flames generally become longer, for cases both with shock waves (Figs. 3a,b,c,f) and without shock waves (Figs. 3d,e,h).

The schematic of a supersonic flame with shock wave interaction is in Fig. 3. The bluff-body stabilized flame has two recirculation zones[18]; the inner recirculation zone shown is driven by the fuel jet while the other zone has recirculation in the opposite direction and is driven by the air flow. As seen in the schematic, the wedge produces a primary shock which reflects off the centerline and interacts with the upstream portion of the flame, near the liftoff location. Downstream of the wedge, the interaction of the supersonic flow with the wedge creates an expansion fan. The expansion fan extends from this beginning ray to a uniform flow region. On the other edge of the uniform flow region is a recirculation zone whose extent can be estimated from the previous result[19]. A second set of shock waves that form are called the recompression shocks. This recompression shock is introduced by the wall and turns the flow once again so that it proceeds directly down the combustor wall.

The wedge downstream corner forms expansion waves which direct the air toward the tunnel sidewalls and the highly curved recompression shocks realign the flow in the axial direction. In Fig. 3j a small Mach disk appears in the primary shock pattern, while Figure 3c shows that a Mach disk can also occur in the recompression shocks within the flame. The primary shock waves extend to the centerline within the flames shown in Figures 3b and 3c, for example, indicating that with combustion most of the flow downstream of the recirculation zone is supersonic.

Shock waves have a dramatic effect on the shapes of the flames. A neck region (i.e., a minimum flame diameter) occurs in the flame shown in Fig. 3b due to the radial inflow caused by the shock waves. The recompression shocks tend to distort and split the flame in Figure 3c and they create a large bulge in the flame tip in Figure 3f, probably due to shock-induced radial outflow. The recompression shocks play an important role to shorten flame lengths by enhancing the mixing and combustion of the unburned mixture in a downstream region. These enhancements are possible due to strong shocks near the centerline location where the recompression shocks intersect. These strong shocks, sometimes become Mach disks, can enhance mixing by generating shock-induced vorticity, and enhance combustion by increasing the local density, pressure and temperature of the mixture and thereby by increasing local reaction rate. The location where the recompression shocks intersect the centerline appears to move upstream as the fuel mass flowrate is increased.

Figure 3g illustrates the flame observed at the onset of thermal choking when two relatively strong

shocks were used. Two 15° wedges (wedge 2) were located at X = 2.8 cm (4.0d_F, mid-upstream) as shown; the flame base is observed to move upstream and it surrounds the fuel tube, leading to dangerously high heat transfer rates. The schlieren image in Fig. 3g indicates that the flow is still supersonic, as evidenced by the shock waves. Further increase in the fuel flowrate causes a strong normal shock to move upstream into the wind tunnel nozzle, and the flow becomes subsonic in the combustor. The fuel tube oscillates in space due to sonic buffeting caused by unsteady shock separation of the wall boundary layers.

Figure 4 shows the effect of combustion on the wall static pressure distributions. With heat release due to combustion, wall static pressures are always greater than that of no combustion case. With combustion, wedge affects the wall static pressure distributions in the upstream region and in the downstream region in a different manner. In the upstream region (X_{wedge}/d_F < 10), pressures with wedge are greater; while in the downstream region (X_{wedge}/d_F > 10), pressures with wedge are lower. This can be explained as follows. The most important factor affecting the wall static pressure is the rate of heat release per unit length (dQ/dx), the absolute magnitude of which is determined by the mean flow velocity and the reaction rate. In the upstream region, dQ/dx is higher for wedge case due to decreased flow velocity and maybe due to shock-increased reaction rate. The different heat release patterns with and without wedge can be explained by comparing the direct photographs in Figs. 3b and 3d.

Figure 5 presents pitot pressure data with no combustion. Fuel injection has almost no effect on the pitot pressure distributions, while wedge slightly affects the pitot pressures. The effects of combustion (heat release) on the pitot pressure distributions are shown in Fig. 6. Heat release increases the pitot pressures near wall, while in the center (within the flame) heat release tends to decrease the pitot pressures. However, the effects of heat release on the pitot pressure distributions are not clear.

Flame Lengths

Flame lengths are measured to quantify the effect of shock waves (wedge) on the overall fuel-air mixing rates. Figure 7 shows lengths of supersonic flames measured from digitized images, with and without shock waves for different wedge positions and wedge angles. Flame length is defined as the distance from the fuel injector to the farthest downstream location where the intensity of the digitized image of the flame decreases to 30% of the maximum intensity recorded in the flame. The positive slope of the curves of flame length versus fuel flowrate in Fig. 7 is similar to previous findings in our laboratory for supersonic flames with no shock waves[4]; similarly, a positive slope also is reported for subsonic flames with coaxial air[20]. With

coaxial air present, larger fuel flowrates generally require a longer distance to consume the fuel[20]. In contrast, the length of a turbulent jet flame with no coaxial air is independent of fuel flowrate because the mixing rate increases linearly with the fuel flowrate.

One major effect of interacting a shock wave with the flame is a significant reduction in the flame length, as shown by the data plotted in Fig. 7. The shortening of the flame also is shown by comparing Figures 3f and 3h, for example. Increasing the wedge angle (shock strength) results in a further shortening of the flames; however, sometimes thermal choking occurs for the stronger shock (15° or 20° wedges). Figure 7 also shows the liftoff heights on centerline that were measured from digitized images. The flame liftoff height tends to increase as the fuel flowrate is increased. For the lowest fuel flowrate, shown in Fig. 3a, the flame is attached to the fuel tube, but in all other cases the flame base is lifted and stabilized within (or downstream of) the air-driven recirculation zone.

In order to decide the best wedge location, lengths of supersonic flames with four different wedge locations are plotted in Fig. 8, for the wedge 1 (10° wedge). From Fig. 8, it is concluded that either upstream position (X_{wedge}/d_F = 1.0) or mid-upstream position (X_{wedge}/d_F = 4.0) is the best wedge location to shorten the flame lengths, thereby enhance the overall fuel-air mixing rate.

Flame Stability Limits

Shock waves have a pronounced effect on the flame stability limits that are plotted in Fig. 9. The hydrogen mass weighted velocity is defined as the hydrogen mass flowrate divided by $\rho_{F,ref}(\pi/4) d_F^2$, where $\rho_{F,ref}$ is the density of fuel at the sonic fuel injector exit for the reference condition for which the fuel stagnation pressure and temperature are 3.7 atm and 294 K. In this study, $\rho_{F,ref}$ equals 0.026 kg/m^3. The mass weighted velocities are used because blowout limits are found to depend on both the velocities and densities of the fuel and air, and because mass flowrates are accurately measured while velocities must be inferred. The actual fuel exit velocity U_F equals the mass weighted value at the reference condition, but the two differ at other conditions. The air mass weighted velocity is the mass flow of air divided by $\rho_{A,ref} A_A$ where A_A is the combustor cross section (18.9 cm^2) at the fuel injector and $\rho_{A,ref}$ is 1.08 kg/m^3.

Figure 9 describes the effects of shock waves on flame stability limits. In Fig. 9, the location of wedge (shock) was varied to understand the effect of wedge location on the flame stability limits. Previous work in our lab[3] has shown that with no shock waves, stability limits of supersonic flames are similar in shape to those of subsonic bluff-body flames and swirl-stabilized

flames[17-19] which also contain recirculation zones. Three blowout limits usually exist, corresponding to a maximum fuel flowrate, a minimum fuel flowrate, and a maximum air flowrate. Figure 9 quantifies the minimum fuel blowout limit for the no wedge case. It was not possible to achieve a maximum fuel flowrate or a maximum air flowrate for the no wedge case due to limited gas supplies, so the dashed lines indicate the maximum fuel and air mass weighted velocities at which stable flames were achieved. Increasing the shock strength (wedge angle) decreases the thermal choking limit and the minimum fuel blowout limit. It is concluded that shock waves significantly stabilize the flame by reducing the minimum fuel blowout limit in Fig. 9. The 10° wedge shock sufficiently stabilizes the flame in Figure 3a such that it is not lifted, yet with no shock waves the same flame blows out. The shock waves (and wedges) also reduce the maximum fuel flowrate, which is the upper boundary of the stable regions in Fig. 9. However, this thermal choking limit is a facility-dependent limit rather than a general limit.

It is concluded that shock waves significantly stabilize the flame by reducing the minimum fuel blowout limit in Fig. 9. Since the present flames cannot be stabilized unless there is a sufficiently large bluff-body recirculation zone[3], it follows that the improved stability caused by the shock waves results from some type of interaction between the recirculation zone and the shocks. The strong adverse pressure gradient caused by primary shocks and wedges can create a recirculation zone in a boundary layer, for example; and shock waves can increase the size of an existing recirculation zone, as shown by Winterfeld[2]. The shocks also can raise the temperature of the recirculated gas. Vorticity created by the shock[1] also may aid in enhancing mixing and flame stabilization.

The optimum strength and location of wedges were investigated by mounting the 10°, 15° and 20° wedges at various axial locations: $X_{wedge} = 1.0$ d_F, 4.0 d_F, 8.5 d_F, and 11.5 d_F. The cost paid for the total pressure loss encountered and the improvement in mixing and flame stability limits were considered together. Based on this criteria, the best mixing and stability corresponds to 10° wedges placed at an upstream position (4.0 d_F) such that the primary shocks create radial inflow near the flame base and interact with the recirculation zone. This upstream wedge position also allowed the second set of shocks (recompression shocks) to provide radial inflow near the flame tip. Lu and Wu[21] also suggested an upstream position as the best wedge location in their nonreacting flow simulation.

Conclusions

Measured shock effects were investigated by changing shock strength and position with particular emphasis on the lengths and stability limits of supersonic hydrogen-air jet flames. Static pressures, pitot pressures, flame lengths, flame stability limits (flame blowout limits and thermal choking limits), shapes of flames, and schlieren visualization pictures were measured and compared to corresponding flames without shock-flame interaction.

The major conclusions of the present study are as follows:

1. Shock waves significantly alter the shape, visible length, and blowout limits of a supersonic jet flame as shown by Schlieren and direct photographs. Shock strength was varied, as well as the hydrogen flowrate and the location of the shock-flame interaction.

2. Shock waves enhance overall mixing rates, since flame length decreased by approximately 30% when shocks were added. One reason for this enhancement was that the present shocks imparted a radial inflow velocity to the air at an intermediate axial location, and imparted a radial outflow velocity to the fuel and air mixture near the flame tip. Both of these effects are believed to improve mixing. The effects of other mechanisms, including the vorticity generation predicted by Marble, cannot yet be determined.

3. Shock waves greatly enhance one of the flame stability limits, namely the blowout limit that is associated with a minimum fuel velocity. One explanation is that the adverse pressure gradient caused by the shock can enlarge the subsonic recirculation zone behind the flameholder.

4. Shock waves (and/or the wedges used to create shocks) have an adverse effect on another flame stability limit, namely the maximum fuel velocity limit prior to thermal choking. Photographs show that thermal choking, which is purposely used in "dual mode" scramjet operations, causes the present flames to move upstream and surround the flameholder, leading to dangerous heat transfer rates.

5. Optimization of the mixing and stability limits requires a careful matching of the shock-flame interaction location, the shock strength, the flame length, and the geometry of the recirculation zone/wake of the flameholder. Best results occur if (1) the primary shocks are positioned to interact with the flame base and (2) the downstream recompression shocks, determined by the wedge placement and size, interact with the central portion of the flame. The experimental results show

that the best mixing and stability corresponds to 10° wedges placed at an upstream position (4.0 d$_F$).

Acknowledgements

References

[1]Marble, F.E., "Gasdynamic Enhancement of Non-Premixed Combustion," *Twenty-Fifth Symposium (International) on Combustion*, The Combustion Institute, Pittsburgh, 1994, pp. 1-12.

[2]Winterfeld, G., "On the Burning Limits of Flameholder Stabilized Flames in Supersonic Flow", AGARD CP 34, Part 2, 1968, pp. 28-1 to 28-12,.

[3]Yoon, Y., Donbar, J., and Driscoll, J. F., "Blowout Stability Limits of a Hydrogen Jet Flame in a Supersonic, Heated, Coflowing Air Stream," *Comb. Sci. Tech.* 97, 1994, pp.137-156.

[4]Driscoll, J.F., Huh, H., Yoon, Y. and Donbar, J., "Measured Lengths of Supersonic Hydrogen Air Flames," to appear in *Combust. Flame*, 1996.

[5]Menon, S., "Shock-Wave-Induced Mixing Enhancement in Scramjet Combustors" AIAA Paper 89-0104, 1989.

[6]Drummond, J.P., Carpenter, M. H., and Riggins, D.W., "Mixing and Mixing Enhancement in Supersonic Reacting Flowfields," Chpt. 7 in *High Speed Flight Propulsion Systems*, Prog. in Astron. and Aeron. Vol. 137, 1991.

[7]Yang, J., Kubota, T. and Zukoski, E.E., "Application of Shock-Induced Mixing to Supersonic Combustion," *AIAA Journal*, Vol. 31, No. 5, 1993, pp. 854-862.

[8]Jacobs, J.W., "Shock-Induced Mixing of a Light-Gas Cylinder," *J. Fluid Mech.* Vol. 234, 1992, pp. 629-649.

[9]Waitz, I.A., Marble, F.E., and Zukoski, E.E., "Vorticity Generation by Contoured Wall Injectors," AIAA Paper 92-0625, 1992.

[10]Ecklund, D.R., Northam, G.B., and Fletcher, D.G., AIAA Paper 90-2360, 1990.

[11] Cetegen, B.M, and Hermanson, J.C., "Mixing Characteristics of Compressible Vortex Rings Interacting With Normal Shock Waves," *Combust. Flame* 100, 1995, pp. 232-238.

[12] Heister, S.D. and Karagozian, A. R., *AIAA J.* Vol. 28, No. 5, 1990, pp. 819-827.

[13]Cheuch, S.G., Lai, M.-C., and Faeth, G.M., "Structure of Turbulent Sonic Under-expanded Free Jets," *AIAA J.* Vol. 27, No. 5, 1989, pp. 549-559.

[14]Glawe, D.D., Donbar, J. M., Nejad, A.S. Sekar, B. Chen, T.-H., Samimy, M. and Driscoll, J. F., "Parallel Fuel Injection from the Base of an Extended Strut into Supersonic Flow," AIAA Paper 94-0711, 1994.

[15]Barlow, R.S., Fourguette, D.C., Mungal, M.G., and Dibble, R.W., "Structure of a Supersonic Reacting Jet," AIAA Paper 91-0376, 1991.

[16]Cheng, T.S., Wehrmeyer, J.A., Pitz, R.W., Jarrett, Jr., O., Northam, G.B., *Combust. Flame* Vol. 99, 1994, pp. 157-173.

[17]Chen, R.H., Driscoll, J. F., Kelly, J., Namazian, M. and Schefer, R.W., *Combust. Sci. Tech.* Vol. 71, No. 4, 1990, pp. 197-217.

[18]Feikema, D., Chen, R.-H., and Driscoll, J. F., "Effect of Swirl on the Enhancement of Flame Blowout Limits," *Combust. Flame* Vol. 80, 1990, pp. 183-195.

[19]Roshko, A., and Thonke, G.T., "Observations of Turbulent Reattachment Behind an Axisymmetric Downstream-Facing Step in Supersonic Flow," *AIAA J.*, Vol. 4, No. 6, 1966, pp. 975-980.

[20]Feikema, D., Chen, R.-H., and Driscoll, J. F., "Blowout of Nonpremixed Flames: Maximum Coaxial Air Velocities Achievable, With And Without Swirl," *Combust. Flame* Vol. 86, 1991, pp. 347-358.

[21]Lu, P.J. and Wu, K.C., "On the Shock Enhancement of Confined Supersonic Mixing Flows," *Phys. of Fluids A*, Vol. 3, 1991, pp. 3046-3062.
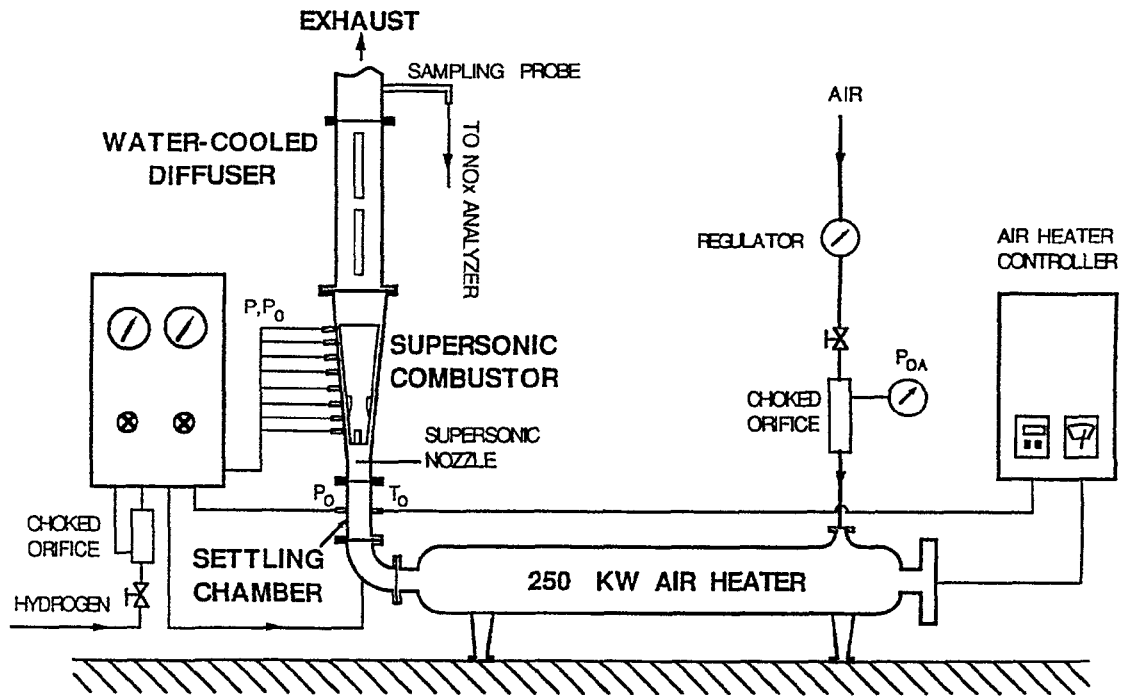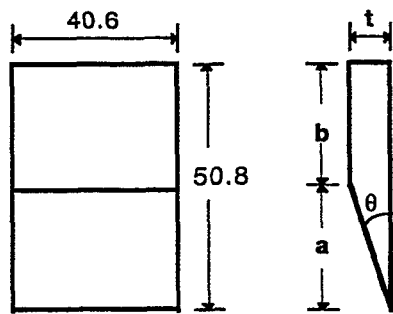
Figure 1 Schematic Diagram of the Supersonic Combustion Tunnel System

[unit: mm]

Table 1   Change of Flow Properties Across the Oblique Shock ($M_1 = 2.5$)

Wedge	Wedge Angle (θ)	Shock Deflection Angle (β)	M_{n1}	P_2/P_1	P_{o2}/P_{o1}	T_2/T_1	M_2
1	10°	31.85°	1.32	1.87	0.98	1.20	2.09
2	15°	36.97°	1.50	2.46	0.93	1.32	1.87
3	20°	42.89°	1.70	3.21	0.86	1.46	1.65

Table 2   Position of Wedge Leading Edge (X_{wedge})

Position	upstream	mid-upstream	mid-downstream	downstream
X_{Wedge}/d_F	1.0	4.0	8.5	11.5

Wedge	θ	a	b	t
1	10°	32.0	18.8	5.6
2	15°	21.0	29.8	5.6
3	20°	15.5	35.3	5.6

Figure 2 Schematic of the Shock-Generating Wedges.

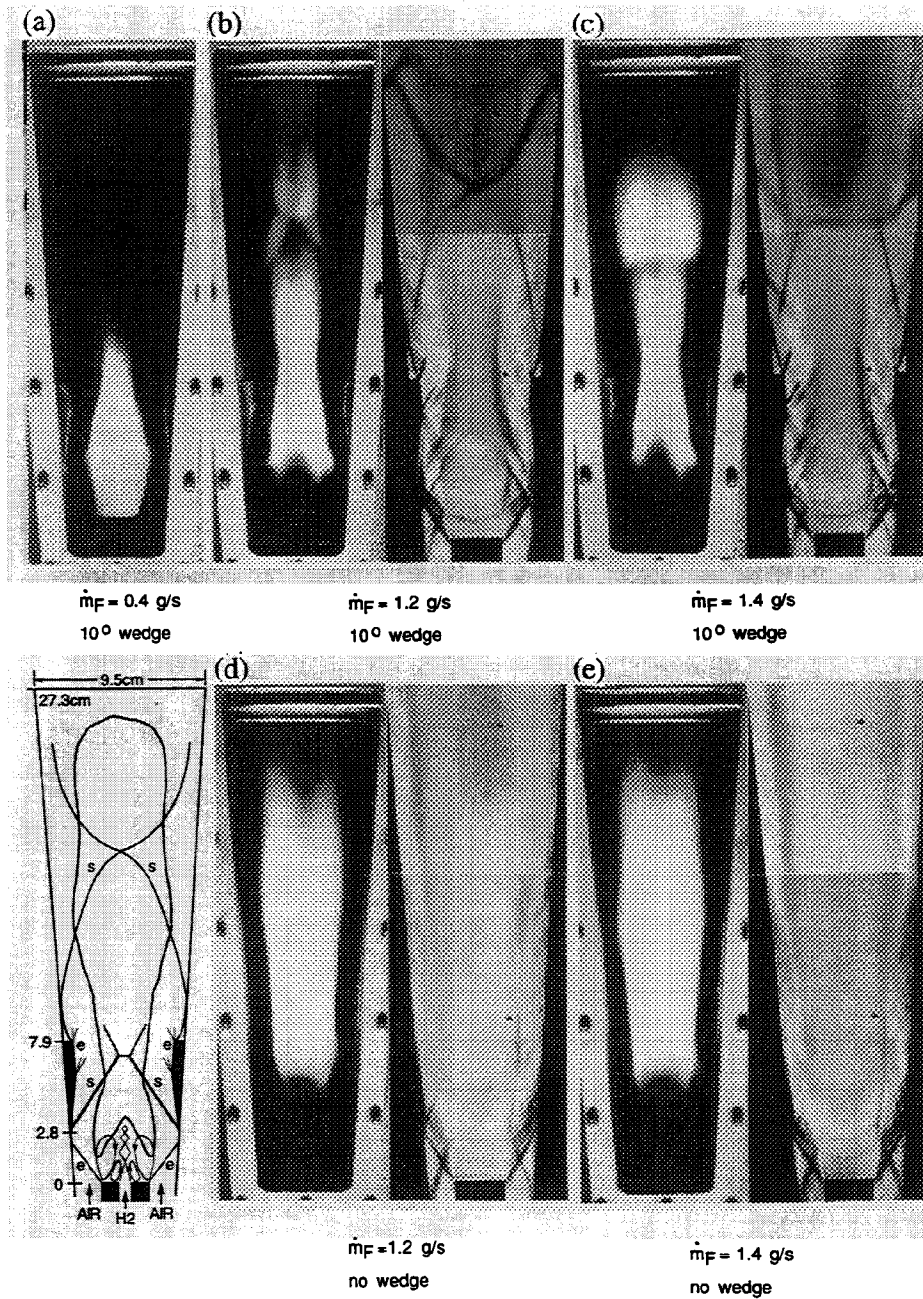American Institute of Aeronautics and Astronautics

Figure 3 Direct and Schlieren Photographs of Supersonic Jet-Like Flames Interacting With Shock Waves (Top Row) and With No Shock Waves (Bottom Row). Window height = 30.5 cm (12 in.). Hydrogen fuel mass flowrate is varied from 0.4 to 1.4 g/s. For the smallest fuel flowrate of 0.4 g/s, the no wedge case is not stable, yet with the wedge the flame is very stable and attached. Distances in schlieren images are 20% larger than in direct photos.
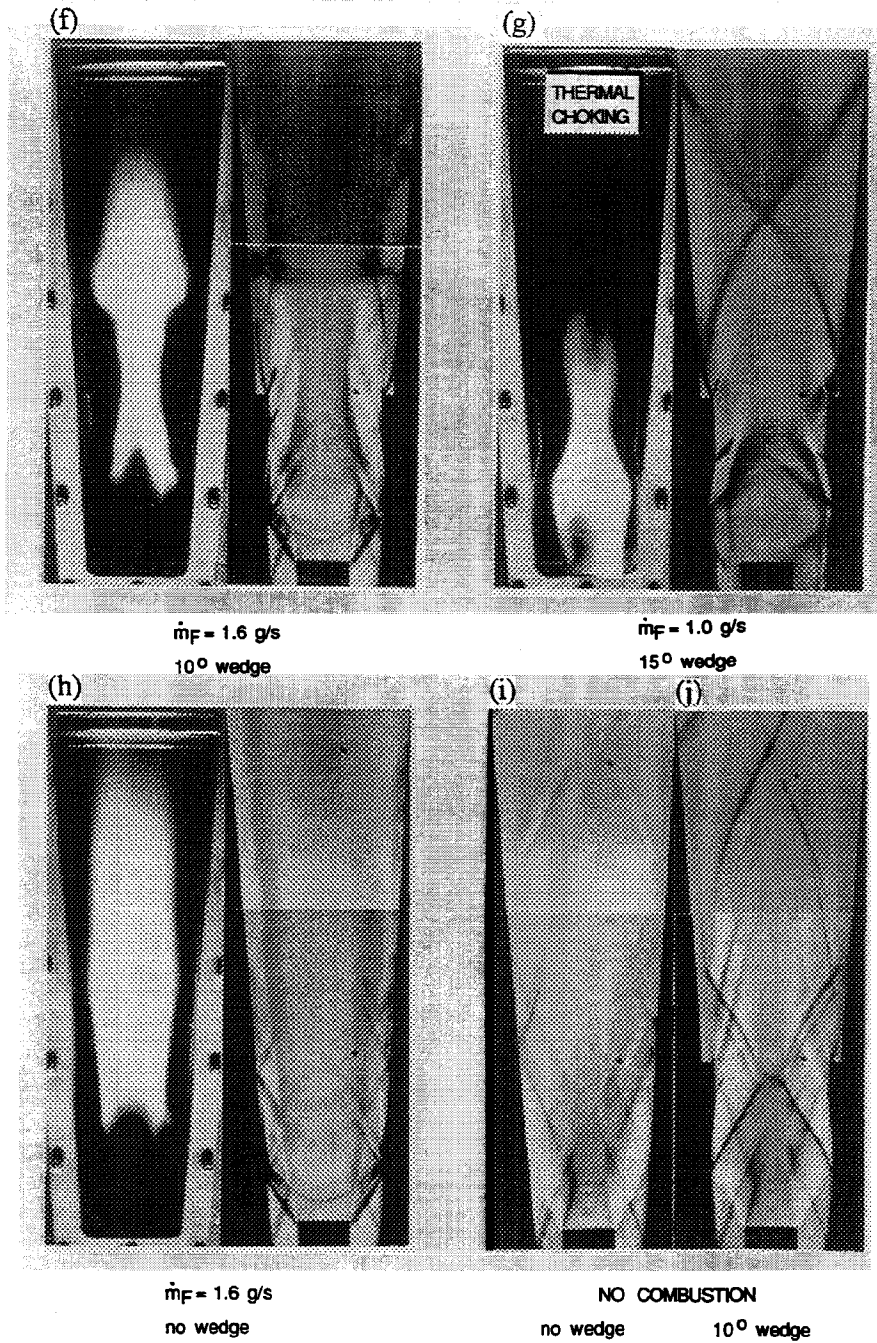
(f)   (g)

$\dot{m}_F = 1.6$ g/s $\dot{m}_F = 1.0$ g/s
10° wedge   15° wedge

(h)   (i)   (j)

$\dot{m}_F = 1.6$ g/s   NO COMBUSTION
no wedge   no wedge   10° wedge

Figure 3   continued. (f), (h): Supersonic Flames For Increased Fuel Flowrates, With and   Without Shock Waves; (g) Onset of Thermal Choking Caused by a 15° Wedge (note that flame moves upstream of fuel injection plane and wraps around the fuel tube); (i), (j): Waves Present With No Combustion.
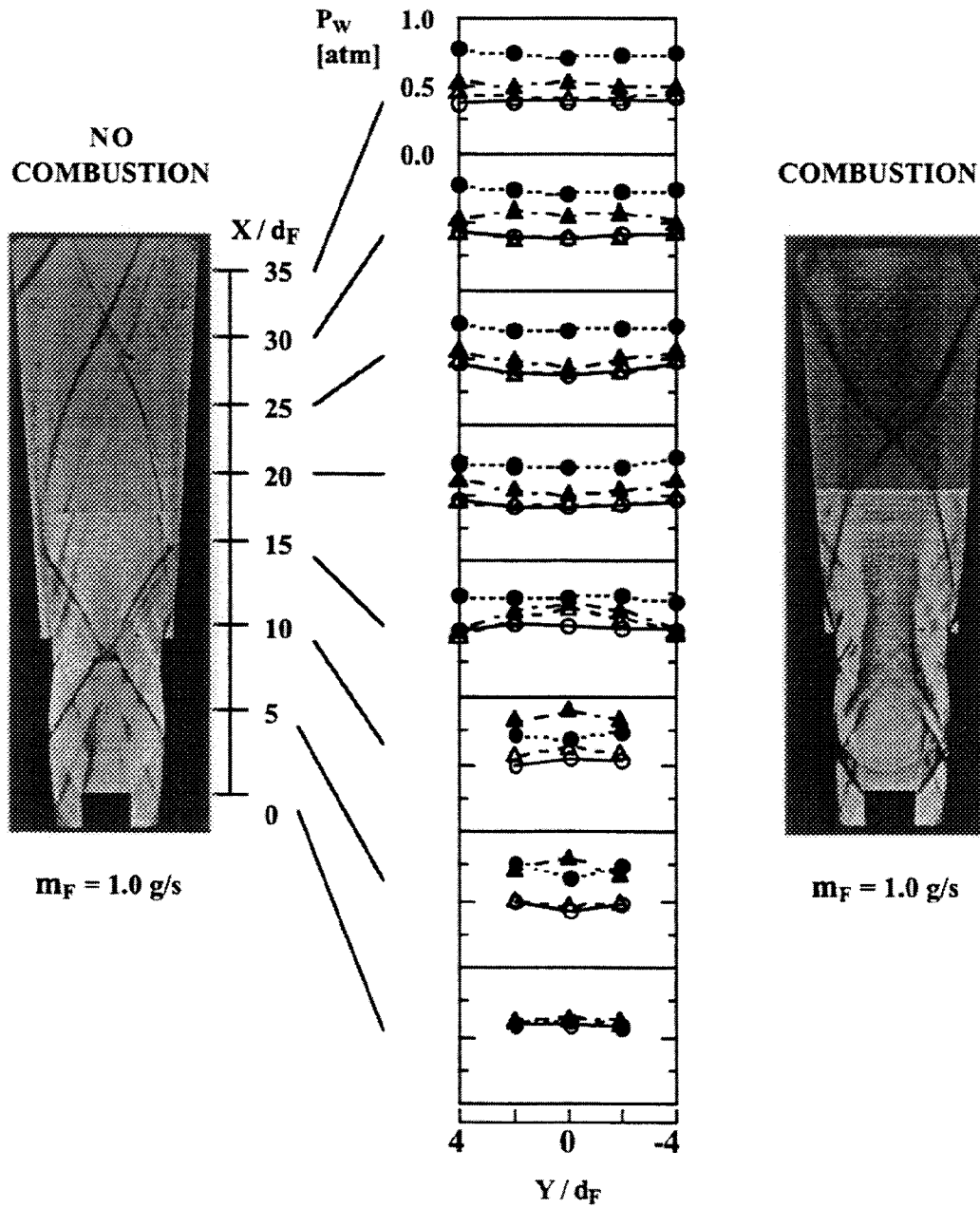
10

Figure 4 . Wall Static Pressure Distribution With and Without Combustion, With and Without Wedge. P_{oA}= 6.44 atm, m_F = 1.0 g/s. O = no wedge, no combustion; Δ = 10° wedge, no combustion; ● = no wedge, combustion; ▲ = 10° wedge, combustion.
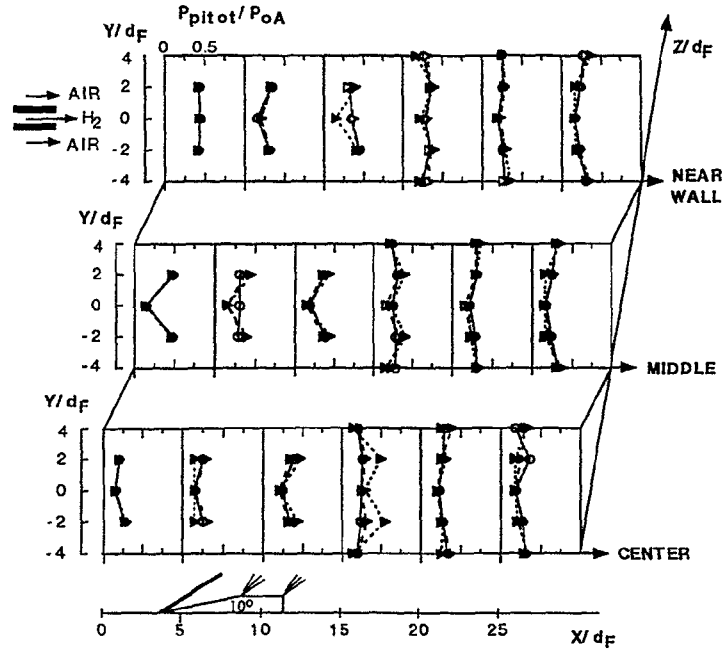
Figure 5   Pitot Pressure Distribution With No Combustion, With and Without Wedge, and With and Without Fuel Injection. $P_{oA} = 6.44$atm, $m_F = 1.0$ g/s. O :no wedge, no fuel ; Δ :no wedge, with fuel; $\blacktriangle$:10° wedge, with Fuel.
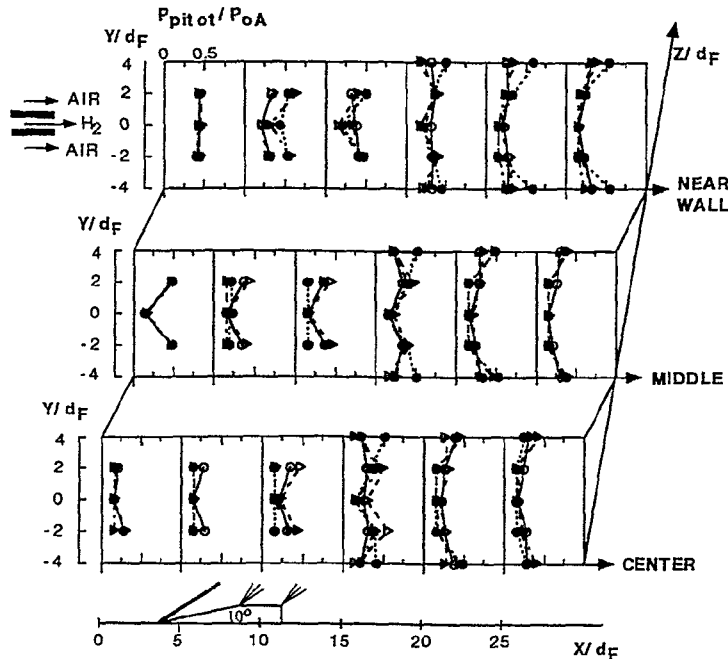
Figure 6   Pitot Pressure Distribution With and Without Combustion, and With and Without Wedge. $P_{oA} = 6.44$atm, $m_F = 1.0$ g/s.   O : no wedge, no combustion ; Δ : 10° wedge, no combustion; $\bullet$: no wedge, with combustion; $\blacktriangle$: 10° wedge, with combustion.

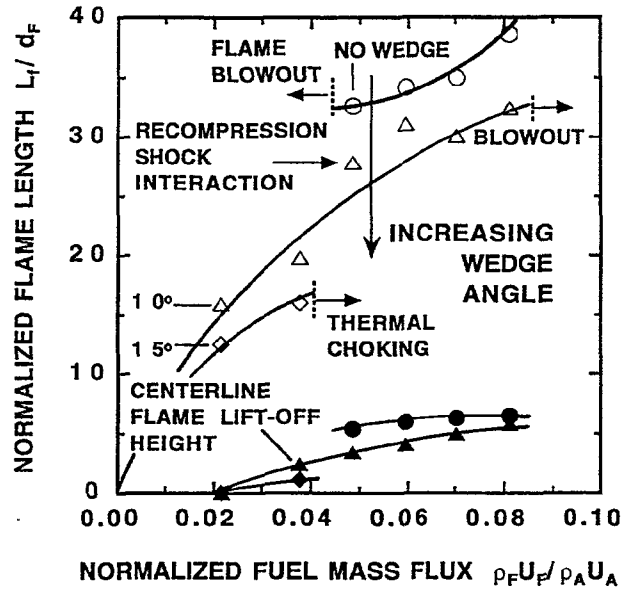12
American Institute of Aeronautics and Astronautics

Figure 7 Lengths of Supersonic Flames Measured From Digitized Images, With and Without Shock Waves for Different Wedge Angles. Also shown are flame lift-off heights on centerline. Air flowrates are constant (0.94 kg/s), fuel flowrates are varied from 0.4 g/s to 1.6 g/s. Fuel inner diameter $d_F = 0.7$cm. Wedges are located at 2.8 cm downstream of the fuel injector plane.
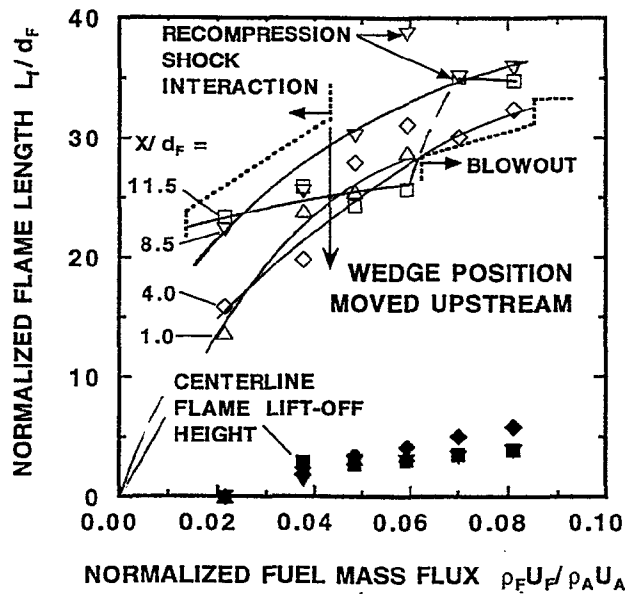

Figure 8   Effect of Wedge Position on the Lengths of Supersonic Flames. $P_{oA} = 6.44$ atm, wedge 1 (10° wedge). Open symbols: L_f, solid symbols: centerline lift-off height.
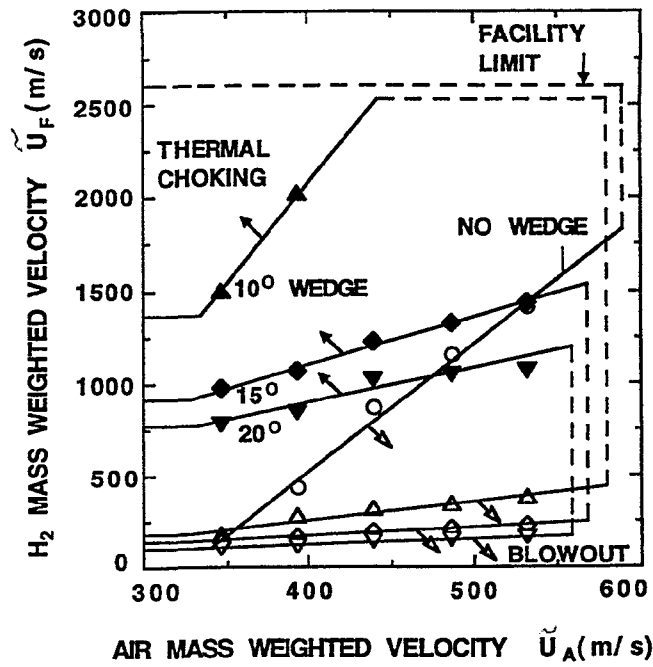
Figure 9 Effect of Shock Strength on the Stability Limits of Supersonic Flames. The lines shown above define four enclosed regions within which stable flames occur. For conditions above the enclosed regions, thermal choking occurs; for conditions below the enclosed regions, blowout occurs. Increasing the wedge angle (shock strength) decreases the thermal choking limit and the blowout limit.

American Institute of Aeronautics and Astronautics